RSC Advances

ROYAL SOCIETY OF CHEMISTRY

www.rsc.org/advances

Development of epoxy mixtures for application in aeronautics and aerospace

Liberata Guadagno[a]*, Marialuigia Raimondo[a], Vittoria Vittoria[a], Luigi Vertuccio[a], Carlo Naddeo[a], Salvatore Russo[b]

Biagio De Vivo[c], Patrizia Lamberti [c], Giovanni Spinelli [c], Vincenzo Tucci [c]

[a]*Dipartimento di Ingegneria Industriale, Università di Salerno, Via Giovanni Paolo II*, 132 – *84084 Fisciano (SA), Italy*

[b] *ALENIA Aeronautica SpA Viale dell'Aeronautica – 80038 Pomigliano D'Arco – (NA), Italy*

[c] *Dipartimento di Ingegneria dell'Informazione, Ingegneria Elettrica e Matematica Applicata, Università di Salerno Via Giovanni Paolo II*, 132– *84084 Fisciano (SA), Italy*

**Corresponding author. Fax +39 089 964057.*

E-mail address: lguadagno@unisa.it

Abstract

This work describes a successful attempt toward the development of composite materials based on nanofilled epoxy resins for the realization of structural aeronautic components providing efficient lightning strike protection. The epoxy matrix is prepared by mixing a tetrafunctional epoxy precursor with a reactive diluent which allows to reduce the moisture content and facilitate the nanofiller dispersion step. The reactive diluent also proves to be beneficial for improving the cure degree of nanofilled epoxy mixtures. It increases the mobility of reactive groups resulting in a higher cure degree than the epoxy precursor alone. This effect is particularly advantageous for nanofilled resins where higher temperature treatments need, compared to the unfilled resin, to reach the same cure degree. As nanofiller, different carbon nanostructured fiber-shaped fillers are embedded in the epoxy matrix with the aim of improving the electrical properties of the resin. The results highlight a strong influence of the nanofiller nature on the electrical properties especially in terms of electrical percolation threshold (EPT) and electrical conductivity beyond the EPT. Among the analyzed nanofillers, the highest electrical conductivity is obtained by using multiwall carbon nanotubes (MWCNTs) and heat-treated carbon nanofibers (CNFs). The achieved results are analyzed by considering the nanofiller morphological parameters and characteristics with respect to the impact on their dispersion effectiveness.

Keywords: Thermosetting polymers, Nanotubes Carbon, Mechanical testing, Reinforced polymers and polymer-based composites, Organic-inorganic hybrid nanostructures.

1. Introduction

The adoption of epoxy-based thermosetting composite materials by the aircraft industry was driven by the increase in performance and most of all by weight reduction. However, composites exhibit some rather poor inherent characteristics, such as low electrical, thermal and mechanical properties. A simple solution to overcome this problem is to modify the matrix molecular structure or add compatible conductive fillers that eventually improve the resulting composite system. In order to choose an effective epoxy mixture, it is necessary to consider that the structure of the resin strongly governs its chemical and some of the physical properties. The number of reactive sites in the epoxy precursors controls the functionality directly acting on the cross-linking density. This, combined with the nature of hardener agent, the functionality, the stoichiometry and the curing cycle determines the final properties of the cured resin especially in terms of mechanical and thermal properties. Conversely, some of the physical properties, such as electrical conductivity can be improved by embedding very small amount of conductive nanoparticles. The use of conductive nanofillers inside polymeric matrices to enhance electrical properties seems to be a very efficient strategy to increase the performance of the composite. In this way when used to form structural parts (e.g. the aircraft fuselage) if a sufficiently high (1-10 S/m) conductivity is reached, the material is able to dissipate lightning currents without employing conductive metal fibers or metal screens which are detrimental in terms of overall weight of the aircraft. Along this stream, in these last few years, various nanofillers or nanostructured conductive materials have been made commercially available which offer a significant chance to reach such a technological goal. By selecting the appropriate resin system with specific nanofillers, critical points in the properties of aeronautic materials might be solved.

Several key factors must be taken into account during the choice of materials for aeronautic applications. In fact, these materials are subject to different environmental conditions such as strong humidity, wide temperature variations, and many types of mechanical stress like compression, tension, torsion and creep. Conventional materials widely used until now include aluminum (density: 2800 Kg/m^3, elastic modulus: 71.7 GPa and temperature limit: 250°C), steel (density: 7830 Kg/m^3, elastic modulus 170 GPa and temperature limit: 1100°C) and titanium (4370 Kg/m^3, elastic modulus 121 GPa and temperature limit: 800°C) [1,2]. However, in this delicate contest of applications, such materials do not allow to achieve a compromise of the requirements that they must satisfy in order to ensure acceptable behavior in terms of corrosion

resistance, low weight, high surface temperature due to the air friction and easy workability, since generally if a property is improved another one is degraded [3]. In order to overcome some of these difficulties, the use of innovative nanocomposites in the aeronautics and aerospace industry has increased significantly in recent years [4, 5].

A detailed review and analysis of their remarkable and superior mechanical, thermal and chemical properties suggests their advantageous replacement to customary materials [6-8].

Also the analysis regarding the electromagnetic properties of the relevant nanocomposites that are of interest to aircraft/aerospace structures reveals the feasibility of their usage for both the efficient lightning strike protection and the design of new electromagnetic shields and radar-absorbing laminates. [9,10].

Among the nanofillers for the production of the nanocomposites, a particular attention has been addressed to carbon nanostructured fibre-shaped fillers, as CNTs and CNFs. Indeed, since Iijima's landmark paper in 1991 [11], carbon nanotubes (CNTs) have spurred many researchers on developing advanced CNT composite materials to transfer some of their excellent physical properties to polymeric matrices [12-18]. Actually, CNTs are considered one of the strongest materials known and very promising to manufacture a very versatile class of composites for structural applications. CNTs in polymeric matrices offer the possibility to combine complementary interesting properties. As conductive filler with high aspect ratio, CNTs are more effective than traditional carbon black [19,20] to obtain composite materials with high electrical conductivity at lower filler concentrations [21-23]. CNFs, though not perfect in the structure and less conductive, are fairly more economical than CNTs for manufacturing epoxy-based systems because they are easier to disperse, process and functionalize. Simultaneously they provide mechanical and electrical property enhancements but with a lower overall cost. These composites are increasingly used for aircraft structures and need to be engineered for efficient lightning strike protection to achieve tolerance similar to that of traditional metal-alloys. The aim of this work is positioned in this contest. We have tried to increase the electrical conductivity of a nanofilled epoxy resin tailored to meet specific needs of the aeronautic field. We have chosen carbon fibre-shaped fillers as MWCNTs and CNFs because they have proven to be very effective in improving electrical conductivity of polymeric matrices. In particular, we have examined the properties of a nanofilled resin obtained by dispersing MWCNTs and CNFs inside an epoxy mixture based on a tetrafunctional epoxy precursors, the TetraGlycidyl-MethyleneDiAniline

(TGMDA), cured with 4,4'-diaminodiphenyl sulfone (DDS). This precursor was selected among several solutions because it shows suitable properties for fibrous composites in aerospace applications. Generally, the physical properties of epoxy resins strongly depend on the functionality of the epoxy precursor; a tetrafunctional precursor assures good properties of the cured resin due to the high level of crosslinking density. Unfortunately, this advantage also causes inconveniences resulting from the brittleness and poor resistance to crack propagation. In this paper, the toughness of the tetrafunctional epoxy precursor has been increased by blending the epoxy precursor with a reactive modifier that performs a double function, as flexibilizer and regulator of viscosity for a best dispersion of MWCNTs and CNFs. Preliminary results on the physical properties of unfilled and nanofilled resins appear very promising. In particular, the use of reactive diluent in the epoxy mixture reduces the moisture content, eases the step of nanofiller dispersion and allows to reach higher curing degree compared to the epoxy precursor alone.

The electrical conductivity values obtained for the epoxy mixture filled with two nanofillers are compared to identify the most promising systems and understand the relations between the electric transport property and the morphological characteristics of the materials. In particular, the role of electron tunneling is discussed on the basis of the *dc* conductivity measurements [24-25]. Moreover, the *ac* characteristics are analyzed in the frequency range [0.1, 1000] kHz in order to highlight the effect of the diverse aggregation and dispersion of the adopted fillers inside the matrix. The interpretation of the different performances are congruent with the morphological observations. The properties of the cheaper and easy-to-process CNFs-based composites appear to be promising for the considered aeronautic application.

2. Experimental section

2.1. Materials and sample preparation

The epoxy matrix was prepared by mixing an epoxy precursor (TGMDA) with an epoxy reactive monomer 1,4-Butandioldiglycidylether (BDE) that acts as flexibilizer and reactive diluents.

These resins, both containing an epoxy, were obtained by Sigma-Aldrich. The curing agent investigated for this study is 4,4'-diaminodiphenyl sulfone (DDS).

The MWCNTs (3100 Grade) was obtained from Nanocyl S.A. The specific surface area of both multi-wall carbon nanotubes determined with the BET method is around 250–300 m^2/g, the carbon purity is >95% with a metal oxide impurity <5% as it results by thermogravimetric

analysis (TGA). Transmission electron microscopy (TEM) investigation has shown for the CNTs a diameter around 20 nm.

Instead, CNFs were produced at Applied Sciences Inc. and they were from the Pyrograf III family.

The pristine CNFs are labelled as PR25XTPS1100 where XT indicates the debulked form of the PR25 family, PS indicates the grade produced by pyrolytically stripping the as-produced fiber to remove polyaromatic hydrocarbons from the fiber surface and 1100 is the temperature in the process production. Sample PR25XTPS1100 was thermally treated to 2500°C to provide the sample named PR25XTPS2500.

The epoxy matrix was obtained by mixing TGMDA with BDE monomer at a concentration of 80%: 20% (by wt) epoxide to flexibilizer. DDS was added at a stoichiometric concentration with respect to the epoxy rings. Epoxy blend and DDS were mixed at 120°C and the nanofillers (MWCNTs or CNFs) were added and incorporated into the matrix by using a ultrasonication for 20 minutes *(Hielscher* model UP200S-24KHz high power ultrasonic probe). All the mixtures were cured by a two-stage curing cycles: a first isothermal stage was carried out at the lower temperature of 125°C for 1 hour and the second isothermal stage at higher temperatures up to 180°C or 200°C for 3 hours. The chosen curing cycle meets industrial requirements (the temperature/time of the first step is lower than the second one to facilitate the carbon fiber impregnation before the resin solidification).

The samples are named TGMDA+DDS+BDE(20%)+ CNT(X%)(Y°C) where X is the CNT percentage and Y is the temperature of the second stage.

2.2. Methods

Thermal analysis was performed with a Mettler DSC 822 differential thermal analyzer in a flowing nitrogen atmosphere. The samples were analyzed in the temperature range of -50÷300°C with a scan rate of 10 °C/min.

SEM micrographs were obtained using a Field Emission Scanning Electron Microscope (FESEM, mod. LEO 1525, Carl Zeiss SMT AG, Oberkochen, Germany).

Some of the nanofilled sample sections were cut from the solid samples by a sledge microtome. These slices were etched before the observation by FESEM microscopy. The detailed

descriptions of the etching procedure and the preparation of the samples are provided in the section "Supplementary Information".

TEM images were recorded on high-resolution transmission electron microscopy (HRTEM) JEM-2100 (JEOL, Japan) operating at 100 kV accelerating voltage. Nanofilled cured samples were sectioned by microtome with a section thickness down to 150 nm and collected on a 400 mesh holey carbon-coated copper grid.

Dynamic mechanical analysis (DMA) of the samples were performed with a dynamic mechanical thermo-analyzer (TA instrument-DMA 2980). Solid samples with dimensions 4×10×35 mm were tested by applying a variable flexural deformation in dual cantilever mode. The displacement amplitude was set to 0.1%, whereas the measurements were performed at the frequency of 1 Hz. The range of temperature was from -60°C to 300°C at the scanning rate of 3°C/min.

Water transport properties were analyzed for unfilled and nanofilled resins. The samples were cut into samples with dimensions of 40×20×0.50 mm immediately after the curing cycle and analyzed. The detailed experimental procedure is provided in the section "Supplementary Information".

The measurements of the *dc* volume conductivity were performed on disk-shaped specimens of about 2 mm thickness and 50 mm diameter by using circular metalized electrodes with a diameter of about 22 mm. Equipment and experimental procedure for the electrical measurements are described in the section "Supplementary Information".

3. Results and discussion

3. 1. Choice of the curing cycle

3.1.1. Thermal analysis

The curing cycle was chosen on the base of Differential Scanning Calorimetry (DSC) and DMA results of the unfilled and nanofilled epoxy samples.

3.1.2. Differential Scanning Calorimetry Results.

The cure behavior of the epoxy matrix was studied by DSC. This technique is especially useful for studying the cure of reactive epoxy systems because the curing is accompanied by the liberation of heat. DSC experiments can provide information on reaction rates, cure rates, and cure degree (DC) [26-28]

In this work, DSC has been used for the estimation of the DC of the samples under the assumption that the exothermic heat evolved during cure is proportional to the extent of reaction. This assumption has already been adopted by other authors [29-30]. The DC can be determined from the total heat of reaction (ΔH_T) of the curing reaction and the residual heat of reaction (ΔH_{resid}) of the partially cured epoxy resin as follows:

$$DC = \frac{\Delta H_T - \Delta H_{resid}}{\Delta H_T} \times 100 \qquad (1)$$

To obtain fraction reacted at various temperatures, we have performed a series of isothermal experiments. To secure accurate total ΔH_T values from isothermal studies, dynamic runs were made after the isothermal curing cycle to obtain the residual heat of reaction. The total heat of reaction was considered as follow:

$$\Delta H_T = \Delta H_{iso} + \Delta H_{resid} \qquad (2)$$

where ΔH_{iso} and ΔH_{resid} are the areas under the isothermal and dynamic thermograms, respectively.

In this paper we have analyzed the cure degree of the system TGMDA+DDS and TGMDA+DDS+BDE(20%) after a two stage curing cycle composed of a first step of 125°C for 1 hour and a second step at the higher temperature of 180°C for 3 hours.

The results of calorimetric analysis performed on the two formulations are reported in Fig.1, where we reported the DSC curve of each formulation before (fresh sample) and after the curing cycle (cured sample). A comparison of the DSC traces highlights a reduced ΔH_{resid} for the sample with BDE.

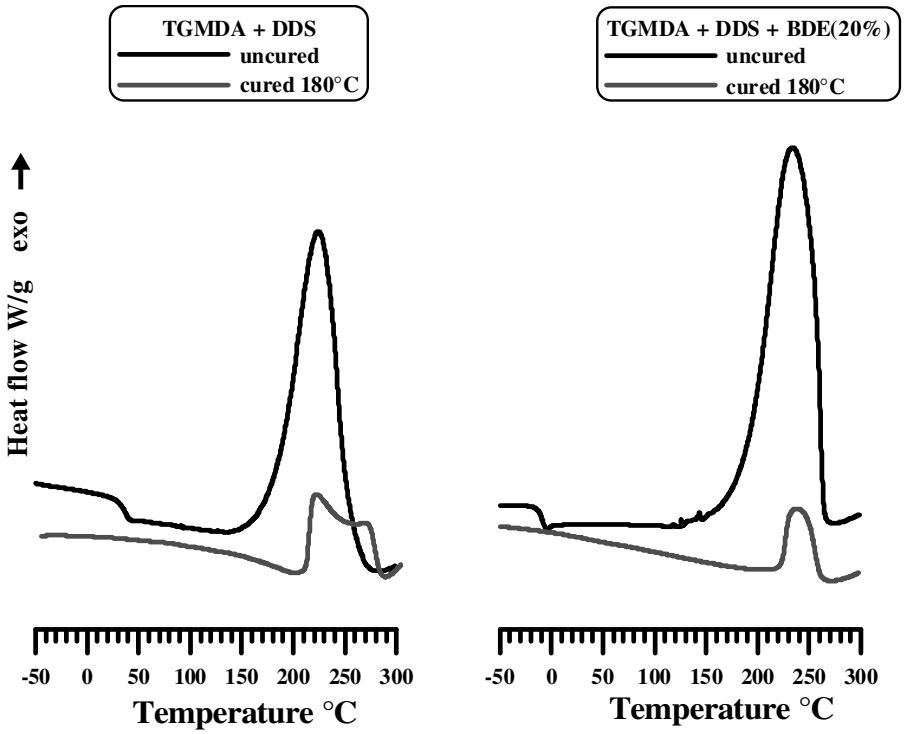

Fig. 1 - DSC curves of: a) the uncured and cured epoxy resin TGMDA+DDS (without reactive diluent) on the left side, and b) the uncured and cured epoxy mixture TGMDA+DDS+BDE(20%)(TGMDA with reactive diluent/DDS) on the right side.

The cure degree for TGMDA+DDS and TGMDA+DDS+BDE(20%) were found to be 80% and 91% respectively. This result has proven that, in the case of TGMDA+DDS+BDE(20%) system, the presence of reactive diluent BDE imparts to the segments of epoxy precursor higher mobility than the epoxy precursor alone; this in turn causes an increases in the efficiency of the curing process increasing the cure degree of about 14% using the same curing cycle.

The inclusion of MWCNTs(0.32%) in the epoxy formulation TGMDA+DDS+BDE(20%) highlighted that this gain is not enough when this formulation also includes MWCNTs. In fact, the DC decreases from 91% to 86% by adding CNTs. To increase the value of the curing degree of the nanofilled formulation, the sample was tested after a curing cycle with the second step at the higher temperature of 200°C for 3 hours. The DC value was found to be 94%, an acceptable value for aeronautic epoxy formulations (see Fig.2). The curing degree for all the nanofilled formulations was always found higher than 92% for the curing cycle with the second step at higher temperature.

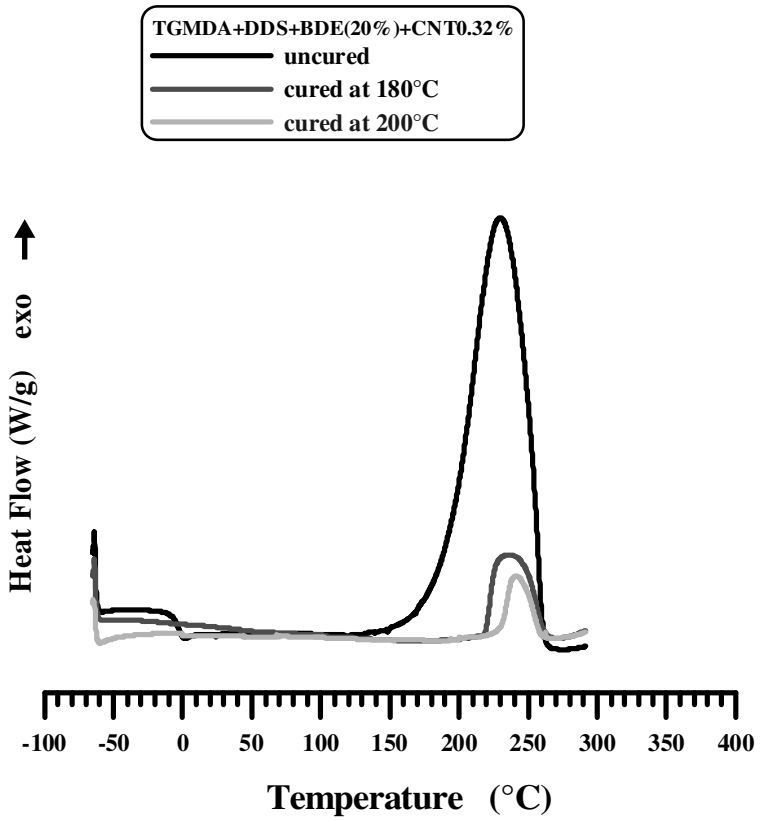

Fig. 2 - DSC curves of: the uncured epoxy mixture TGMDA+DDS+BDE(20%), and the same epoxy mixture cured by two different curing cycles.

Temperatures higher than 220°C are necessary to obtain similar values in same curing degree of nanofilled epoxy mixtures in absence of reactive diluent.

The behavior of the above epoxy formulations were also analyzed using DMA investigation.

3.1.3. Dynamic Mechanical Results

Dynamical mechanical data provide useful information on the relaxation processes that become operative in the polymer in a temperature range depending on the examined system.

The graphics in Fig.3 show that the incorporation of a small concentration of MWCNTs(0.32%) in the temperature range of -60÷180°C causes an increase in the elastic modulus value with respect to the epoxy matrix. The different temperature of the second stage of the curing cycle changes the curve profiles at temperature higher than 70°C. For the lower temperature of the curing cycle (second stage), the nanofilled composite shows a non-progressive decrease in the

value of the elastic modulus with an unforeseen increase between 210 and 240°C before again decreasing. This behavior is very likely due to an increase in the cross-linking density during the heating. This increase is not observed from the pure resin (unfilled sample) with the same history of the curing cycle, see sample TGMDA+DDS+BDE(20%)(180°C). We can explain this behavior if we assume that the inclusion of carbon nanotubes well dispersed inside the matrix causes a reduction of the cross-linking density in a fraction of the epoxy matrix in close contact with the nanofiller. This also explain two peaks in the tan δ of the sample TGMDA+DDS+BDE(20%)+CNT(0.32%)(180°C) indicating the presence of a lower temperature glass transition (at 215°C), beside the main transition at the same temperature as the pristine resin (260°C).

It is very likely that this second lower transition is due to unreacted molecular segments that cause inhomogeneities from regions of varying crosslink density; since the samples TGMDA+DDS+BDE(20%)+CNT(0.32%)(180°C) and TGMDA+DDS+BDE(20%)(180°C) are formulated with the same stoichiometry and curing history, the lower cross-linking density can be ascribed only to the nanoinclusions. This secondary peak, active at a lower temperature disappears for the same composite cured up to 200°C (see sample TGMDA+DDS+BDE(20%)+CNT(0.32%)(200°C)). A more effective curing cycle at higher temperature up to 200°C allows to overcome the drawback due to the inclusion of nanofiller inside the epoxy matrix. It was also observed that a different percentage of MWCNTs is reflected in both the location and magnitude of the transition peak at lower temperature. These results indicate that, for the nanofilled composites, the curing history must to be optimized with respect to the unfilled formulations.

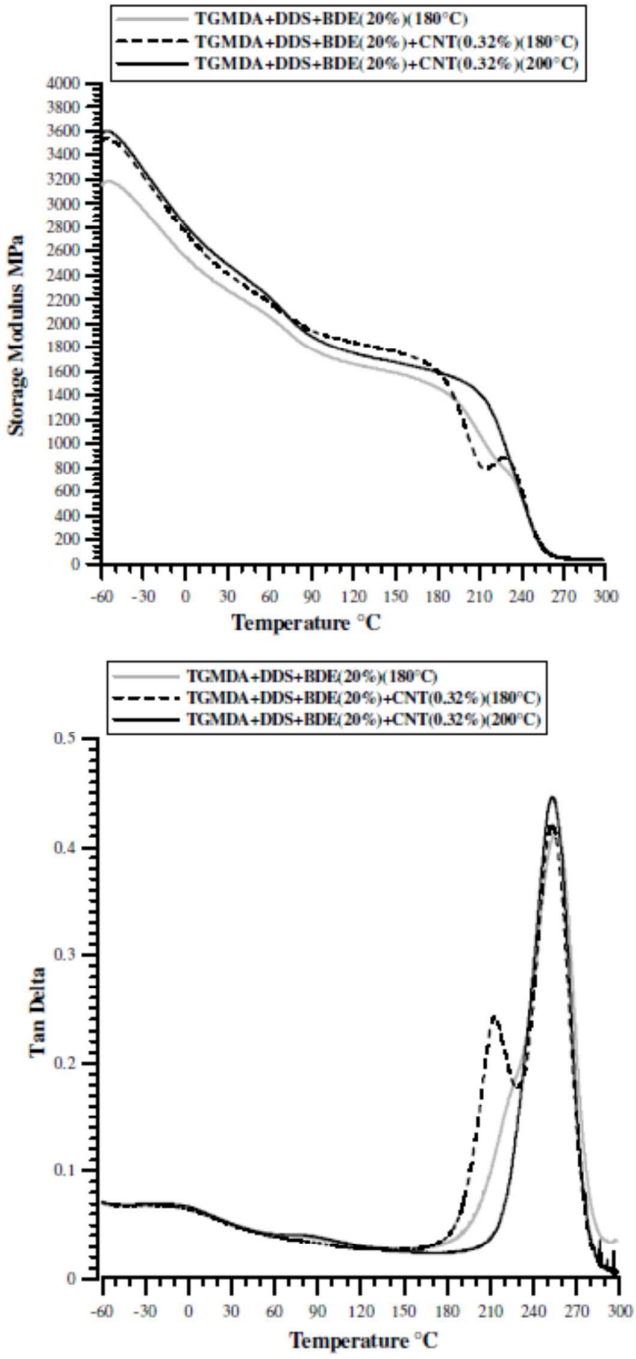

Fig. 3 - Storage modulus (MPa) (at the top), and Loss factor (tanδ) (at the bottom) of the pure epoxy and the composites 0.32 wt% MWCNTs solidified up to 180 and 200°C respectively.

For the reason above described, all the formulations (filled and unfilled) have been cured with a two-stage curing cycle, a first step at 125 for 1 hour and a second step at 200°C for 3 hours.

3.2. Water Transport Properties

Water vapor absorption decreases the performance of aircraft materials for the negative effects on mechanical properties, corrosion and weight. Data concerning the effect of water absorption on the mechanical properties of epoxy resins show a dramatic lowering of the glass transition temperature (Tg) and the consequent degradation of high-temperature properties. Petherick et al. proposed that this depression of Tg is caused by disruption of the strong hydrogen bonds in the cured network, and their replacement with weaker water-related hydrogen bonds [31]. In the field of structural materials for aircraft/aerospace applications more work has been done on the moisture content of TGMDA+DDS system for its properties which allow higher operating temperatures maintaining the mechanical performance. Despite these excellent properties, the water content absorbed is reported to be higher than other common epoxy resins applied as structural resins. In fact, TGMDA+DDS systems (without BDE) are reported to absorb as much as 6.5 wt% water; Liu et al. reported for this system a value of 7.76% (at 23°C) [32] and Li et al. the value of 6.48% (at 35°C) [33]. A higher water content results in a dramatic drop in Tg [34-36].

For our epoxy mixture where a reactive diluent is in the network, no date are available from the literature, therefore we performed measurements of sorption and diffusion of liquid water at 25°C for the unfilled resin (epoxy mixture), the resin with 0.5% of MWCNT, the resin with 0.64% of heat-treated CNFs and the resin with 1% of as-received CNFs. In addition, because the cured samples (without BDE) reported in literature are related to samples hardened with different curing cycles, in this work TGMDA+DDS(200°C) samples (without BDE) cured with the same curing cycle of TGMDA+DDS+BDE(20%)(200°C) epoxy system have been tested and the results are shown in Fig.4 for water activity (a=1) at the temperature of 25°C.

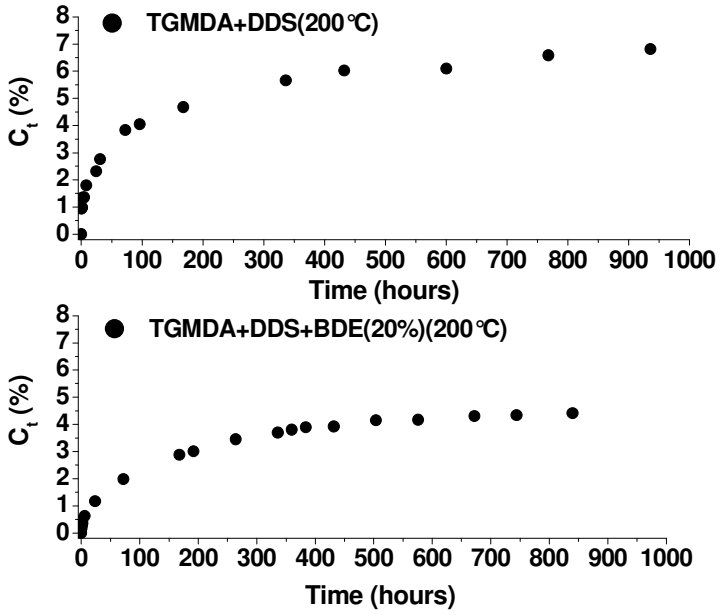

Fig. 4 - The concentration at time (C_t) as a function of the time (hours) of the epoxy resin (without BDE), and the epoxy mixture containing the diluent.

We can see that the presence of reactive diluent in the epoxy mixture reduces the sorption at equilibrium of liquid water (C_{eq}) from 6.81 to 4.41. In conclusion, a percentage of 20 % wt of BDE reduces the value in C_{eq} of about 35%.

The sorption at equilibrium of liquid water C_{eq} into the five samples and the diffusion parameter, D (cm^2/s), are shown in Table 1 while in Fig.5 the reduced curves, C_t/C_{eq}, as a function of square root of time normalized for the thickness *d* of both the unfilled resin and the nanofilled resins are shown. The concentration of water adsorbed at 25℃ is reported as a function of time for samples having the same thickness.

Table 1. Diffusion parameters (D) and Sorption values at equilibrium of liquid water (C_{eq}) of the epoxy resin (without BDE), the epoxy mixture containing the diluent and the nanofilled mixtures.

Sample	C_{eq} (%)	D (cm^2/s)
TGMDA+DDS+BDE(20%)(200℃)	4.41	1.11E-09
TGMDA+DDS(200℃)	6.81	1.29E-09
TGMDA+DDS+BDE(20%)+ PR25XTPS2500(0,64%)(200℃)	5.04	1.25E-09
TGMDA+DDS+BDE(20%)+MWCNT(0,5%)(200℃)	5.25	1.11E-09
TGMDA+DDS+BDE(20%)+PR25XTPS1100(1,0%)(200℃)	4.92	1.35E-09
DGEBA+DDS	4.03	2.00E-09

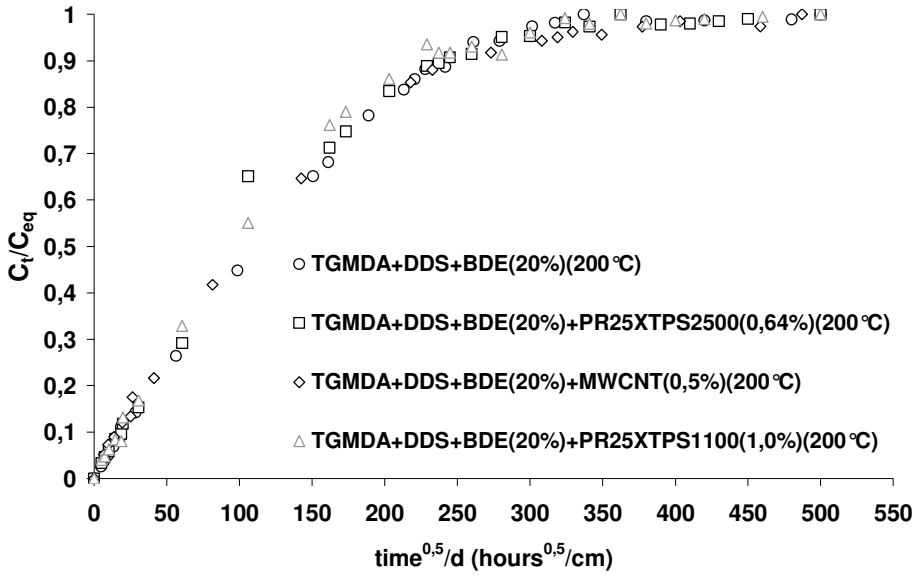

Fig. 5 - C_t/C_{eq} against the square root of time normalized for the thickness d of unfilled and nanofilled mixtures.

Data in Table 1 show that at high water activity (a=1) the nanofilled samples are characterized by values of C_{eq} only slightly higher. This result was already found for a different epoxy matrix, DiGlycidil-Ether Bisphenol-A (DGEBA) cured with DDS at stoichiometric concentration. The thermodynamic interaction of the amorphous resin with liquid water is almost not changed by the presence of the carbon nanotubes and/or heat-treated and untreated CNFs.

The resin is highly plasticized and the most part of water molecules form clusters inside the network. It is worth recalling that, in liquid water, at activity a=1, the plasticizing effect is in the highest degree and hides differences that could be evaluated at lower activity of water. Indeed different behavior was observed for the resin (DGEBA) cured with a different hardener agent and filled with CNT at low water vapor activity [17]. In this paper the aim is to evaluate the difference in the more critical case (a=1) to compare the behavior of this epoxy system with the system without BDE already studied in literature. In Fig. 5, we observe a Fickian behavior, that is a linear dependence of the reduced sorption on square root of time, a curvature for $C_t/C_{eq}>0.7$ and a constant value at equilibrium. This Fickian behavior gives the possibility to derive the diffusion parameter, D, by the first linear part of the curve, by the Eq. (3).

$$\frac{C_t}{C_{eq}} = \frac{4}{d}\left(\frac{Dt}{\pi}\right)^{\frac{1}{2}} \quad (3)$$

where C_{eq} is the equilibrium concentration of water, C_t the concentration at time t, *d* (cm) is the thickness of the sample, and D (cm^2/s) the mean diffusion coefficient. The value of D is between 1.11E-09 and 1.35E-09 cm^2/s. If we consider the very small deviations on the points (attributable to experimental errors), it is evident that the diffusion of water molecules into the samples with different nanofillers follows the same curve. These results lead us to think that the small percentage of nanofiller (max 1%) has no effect on the transport behavior of the samples.

If we compare the results related to the sample TGMDA+DDS+BDE(20%) with data reported for the TGMDA+DDS system (without BDE) we can note that a lower value of absorbed water is obtained for the epoxy mixture TGMDA+DDS+BDE(20%) and also for the nanofilled epoxy resins. This value is almost comparable with the value obtained for DGEBA cured with DDS in stoichiometric amount as we can see for all the analyzed samples in Table 1.

3.3. Thermogravimetric analysis

Thermogravimetric analysis (TGA) can be used to study the oxidative stability of the components and formulated resins. Thermal degradation in air of the unfilled epoxy formulation TGMDA+DDS (without reactive diluent) and the reactive diluent BDE are shown in Fig.6. The unfilled epoxy mixture begins to degrade at 320°C, while the reactive diluent at 120°C. The Fig.7 shows the thermogravimetric curves of the uncured TGMDA+DDS+BDE(20%) formulation together with the curve of the same epoxy mixture after the two step curing cycle, TGMDA+DDS+BDE(20%)(180°) and TGMDA+DDS+BDE(20%)(200°). The curve of the uncured mixture shows at 120°C the beginning of a first step of degradation involving a very small fraction of materials due to the degradation of the reactive diluent. Fortunately, the cured mixture begins to degrade at 320°C which is the temperature at which the epoxy mixture composed of only the epoxy precursor TGMDA starts to degrade. This is a very useful result which also highlights that when the reactive diluent is in the epoxy network, it is thermally stable up to 320°C. The Fig.7, on the right side, also shows the thermogravimetric curves in air of the same epoxy formulation nanofilled with a percentage of 0.32 % of MWCNTs. We can see that

no change in the thermogravimetric curves are shown, as the previous results, in the cured nanofilled formulation, the reactive diluent does not constitute a problem for the thermal stability of the formulation.

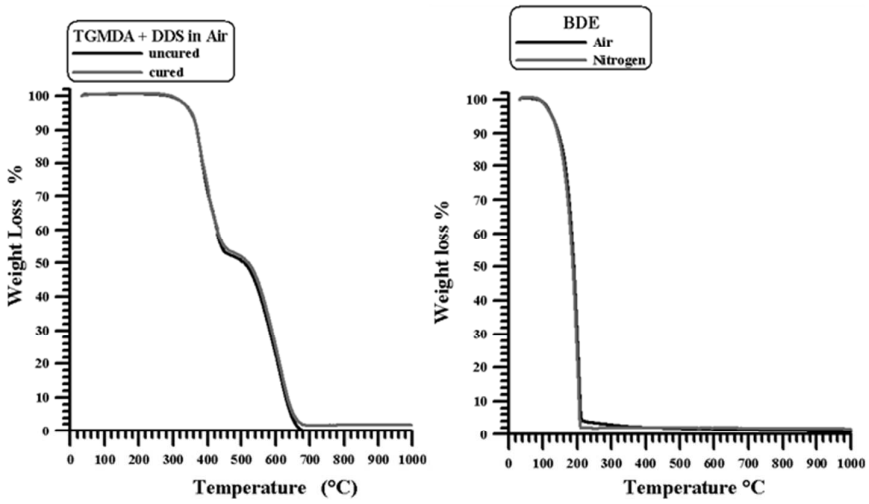

Fig. 6 - Thermogravimetric curves in air of: a) the uncured and cured unfilled epoxy resin TGMDA/DDS (without reactive diluent) on the left side, and b) the reactive diluent BDE on the right side.

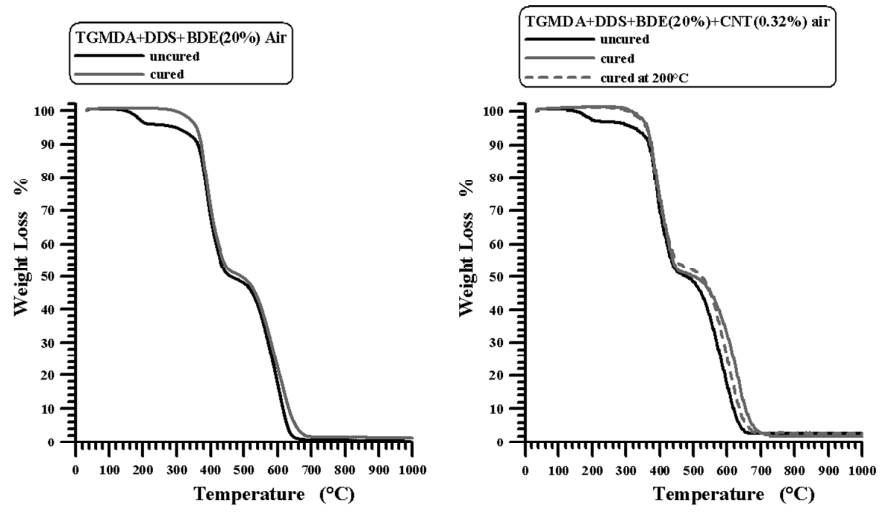

Fig. 7 - Thermogravimetric curves in air of : a) the uncured and cured unfilled epoxy mixture TGMDA+DDS+BDE(20%) (TGMDA with reactive diluent/DDS) on the left side, and b) the same epoxy formulation nanofilled with a percentage of 0.32% of MWCNTs on the right.

Very similar results were obtained for the epoxy resins filled with untreated and heat treated CNFs; in addition, the different thermal treatment of CNFs does not have an appreciable effect on the degradation behaviour. On the contrary, the electrical properties shown in the section 3.3.2 demonstrate the strong influence of the thermal treatment on the conductivity and electrical percolation threshold of the two different samples.

3.4. Morphological investigation

In order to analyze the homogeneity of the nanofiller dispersion in the polymeric matrix, the nanofilled samples with MWCNTs, as received CNFs and heat-treated CNFs were investigated by means SEM. Morphological analysis was carried out on etched samples to remove the resin surrounding the nanofibers, leaving them bare as described in the section "Experimental".

SEM investigation was also carried out to study the dispersion of MWCNTs at different concentration of MWCNTs. Fig. 8 shows SEM images of etched nanofilled epoxy composites after at loading rate of 0.64 (see Fig. 8 – Sample A), 0.32 (see Fig. 8 - Sample B) and 0.05 (see Fig. 8 - Sample C) per cent by weight. A careful observation evidences a homogeneous structure in the samples with nanofiller percentage of 0.64% and 0.32% in which the CNTs are uniformly distributed into the epoxy matrix (see Fig. 8 – Sample A and Fig. 8 – Sample B). In fact, for this CNT percentage, we observe whole lengths of the carbon nanotube segments released from the residual resin fraction Fig. 8 – Sample C shows the fracture surface of the epoxy composite at a nanofiller percentage of 0.05%.

In this sample, the effect of etching procedure generates small "islands" of nanofilled resin which are not interconnected by CNTs as observed in Samples A and B where single nanotubes besides touching each other also create contacts in the whole mass of the sample crossing the areas where the resin was completely removed by the etching procedure. This observation was also confirmed by TEM investigation as it can be seen Fig.9 for Sample B (0.32% of CNTs) which confirmed that single nanotube are distributed along the sample. TEM investigation for the sample filled with a lower percentage of 0.05% (not reported here) confirmed that completely separated nanotubes are embedded in the matrix. In this case the dispersion state is very different with respect to the Samples A and B. In the section of Electrical Behavior we will show that this different dispersion state strongly influence the nature of the electrical interaction between nanotubes inside the epoxy matrix and therefore their conductive paths.

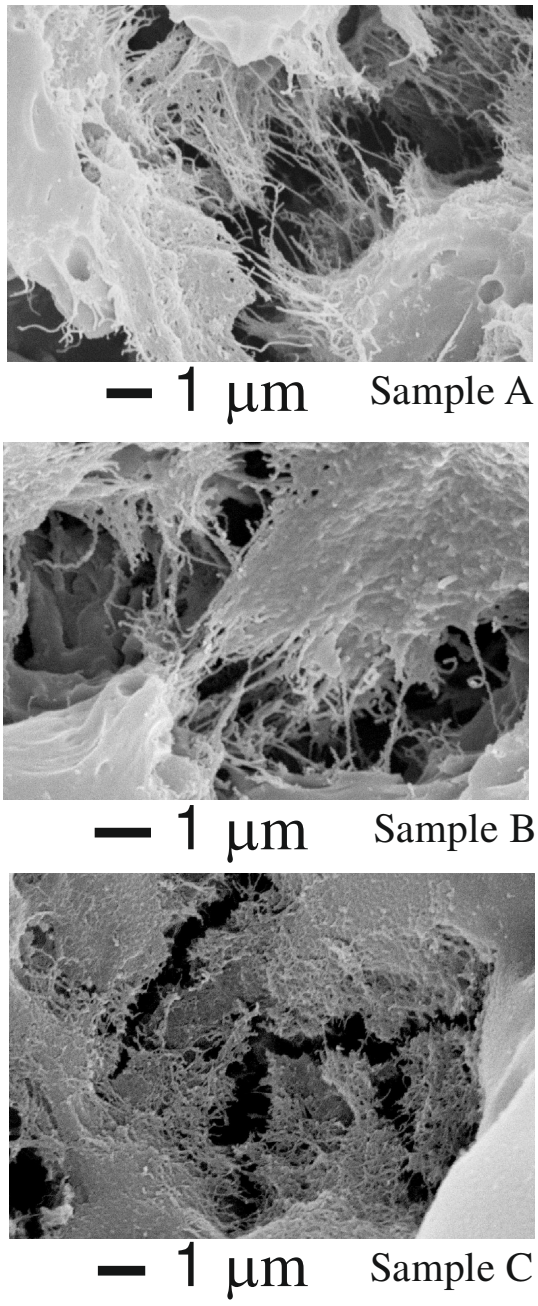

Fig. 8- Fracture surface SEM images of the nanofilled epoxy composites at loading rate of Sample A) 0.64, Sample B) 0.32 and Sample C) 0.05 per cent by weight of CNTs.

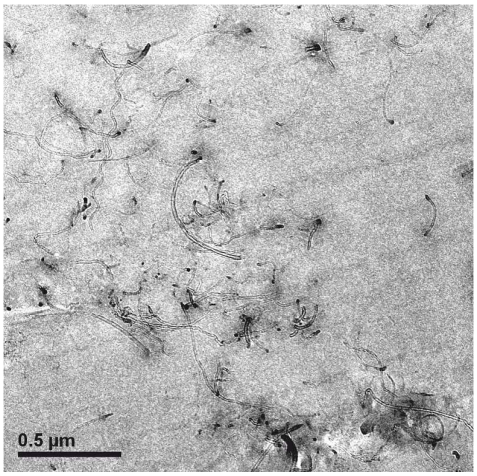

Fig. 9 - TEM image of Sample B (epoxy resin at loading rate of 0.32 per cent by weight of CNTs).

Fig.10 shows SEM images of etched nanofilled epoxy composites at loading rate of 0.64 per cent by weight of CNFs. The as-received CNFs filled composites are on the top and those with heat-treated CNFs are on the bottom.

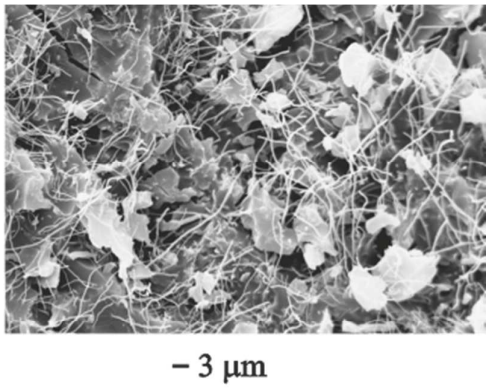

Fig. 10- Fracture surface SEM images of the nanofilled epoxy composites at loading rate of 0.64 per cent by weight: as received CNFs filled resin is on the top, heat-treated CNFs filled resin is on the bottom.

A careful observation of the SEM images seems to highlight the following points (1-4).

1) SEM investigations highlight that CNFs are uniformly distributed in the epoxy matrix in both the samples; in fact they cover the entire surface of the samples where they are even observable as single nanofibers in each zone of the fracture surface. Figs. 8 and 10 also highlight that for the nanocomposite with CNTs, the epoxy matrix is bonded to the nanofiller which tends to form nets; whereas, in the case of CNFs, the different morphological parameters of CNFs determines a better level of nanofiller dispersion that is hard to obtain with other CNTs for which Van der Waals forces are stronger due to their smaller size with respect to CNFs.
2) Heat-treated CNFs seem to be characterized by a more straight structure than un-treated CNFs. This morphological characteristic is most probably due to a more perfect rigid structure which results in a less tendency to bend with respect to untreated CNFs; as expected, the straight morphological feature is statistically observed for all the concentrations of heat-treated CNFs, as it can also be observed in Fig.10 for the samples filled with a higher percentage of CNTs.
3) Heat-treated CNF seems statistically to show a narrowing of the diameter, this effect can be well observed in Fig.11 where the samples filled with untreated and heat-treated CNFs were acquired with the same magnification.
4) Heat-treated CNF seems statistically less bonded to the epoxy matrix; this effect can be also observed in the enlargements of Fig.12, where we can see that, in the case of untreated CNFs, the majority of the CNFs is tightly tied to the epoxy matrix.

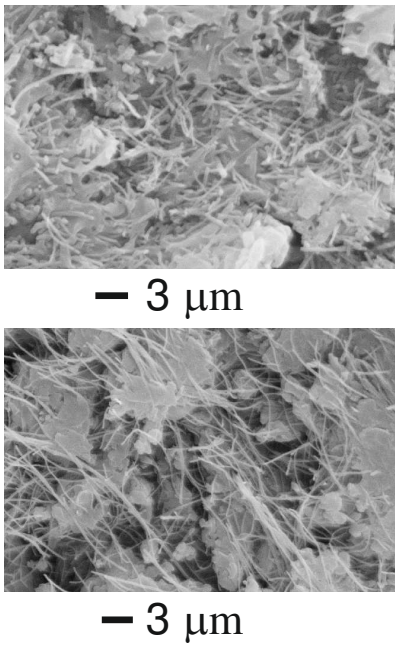

Fig. 11- Fracture surface SEM images of the nanofilled epoxy resins at loading rate of 1% by weight: as received CNFs filled resin is on the top, heat-treated CNFs filled resin is on the bottom.

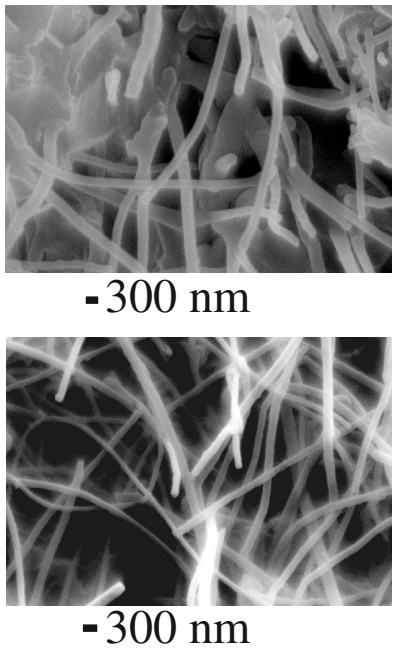

Fig. 12 - Fracture surface SEM images (enlargement) of the nanofilled epoxy resins at loading rate of 1% by weight: as received CNFs filled resin is on the top, heat-treated CNFs filled resin is on the bottom.

The difference in the interaction CNF-matrix can be understood considering the analysis performed on the effect of heat-treatments on CNFs in previous papers [37-38].

In particular, Endo et al. to understand the effect of heat treatment on the nanofibers performed different tests using various analytic techniques, such as high-resolution transmission electron microscopy (HRTEM), Raman spectroscopy, X-ray diffraction and the electrical conductivity in the bulk state [37].

They found that the untreated CNF shows a morphology, termed "stacked cup" that generates a fiber with carbon planes' exposed edges along the entire interior and exterior surfaces of the nanofiber. The most prominent feature upon heat treatment of these nanofibers is the formation of energetically stable loops between adjacent active end planes both on the inner and outer surfaces.

These loops can contribute to round the walls, thus eliminating the exposed edges. Guadagno et al., analyzing Fourier transform infrared spectroscopy (FTIR) of untreated and heat-treated CNFs, found that a less number of chemical groups are attached on the wall of heat-treated CNFs. These groups, more numerous on the wall of un-treated CNFs, are most probably responsible of covalent and/or non-covalent bonds such as intermolecular forces due to hydrogen bonds. It was found that these stronger interactions also favor the mechanical reinforcement.

The stronger interaction of un-treated CNF with the matrix than the heat treated CNF could be due to a synergic combination of these two effects: on the one hand the carbon planes' exposed edges of the untreated CNFs and on the other hand the number of functional groups attached to the walls of the nanofibers. These groups (most of all hydroxyl and ether groups) are available for chemical and physical interactions between the walls and the epoxy matrix.

3.5. Electrical Behavior

3.5.1. DC conductivity of nanofilled resins

Fig.13 shows the *dc* volume conductivity of the composite as a function of filler loading (%wt). The results obtained, for the composite with MWCNT and heat-treated CNFs, above the percolation threshold are among the highest values obtained for epoxy systems [39].

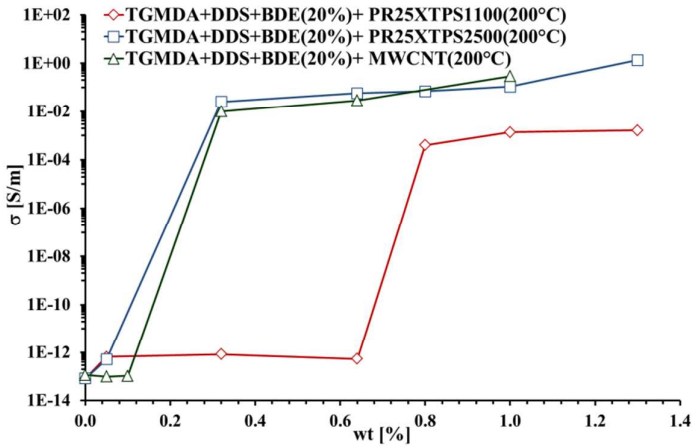

Fig. 13 - DC volume conductivity of the nanofilled composites as a function of the nanofiller concentration.

At low filler contents, the composite exhibits an electrical conductivity comparable to that of the pure polymer. Instead, near the percolation threshold, which, as evident from Fig. 13 is different for the diverse systems, the composite exhibits a transition from an insulating to a conducting behavior. At higher filler concentrations the electrical conductivity reaches a plateau at a value several orders (generally more than four/five) of magnitude above that the neat resin.

The dependence of the conductivity of the carbon-based filled composites above the percolation threshold as a function of the filler concentration is described by the classical power law [18,22,40-42]. $\sigma = \sigma_0(\phi - \phi_c)^t$ where σ_0 is the intrinsic conductivity of the filler, ϕ is the filler concentration (in weight or volume fraction), ϕ_c is the percolation threshold and t an exponent depending on the dimensionality of the percolating structure.

If the filler content in the composite is homogenous, the composite conductivity, above the percolation threshold, can be described by the behavior of a single tunnel junction. This suggests the DC conductivity should follow the following expression [24-25,43] :

$$\ln(\sigma_{DC}) \propto \phi^{-1/3} \qquad (4)$$

The detection of a linear relation between the DC conductivity (in logarithmic scale) and $\phi^{-1/3}$, as shown in Fig.14, is a classic approach adopted to confirm that electron tunneling is the main responsible for the electrical conductivity in such nanofilled resins.

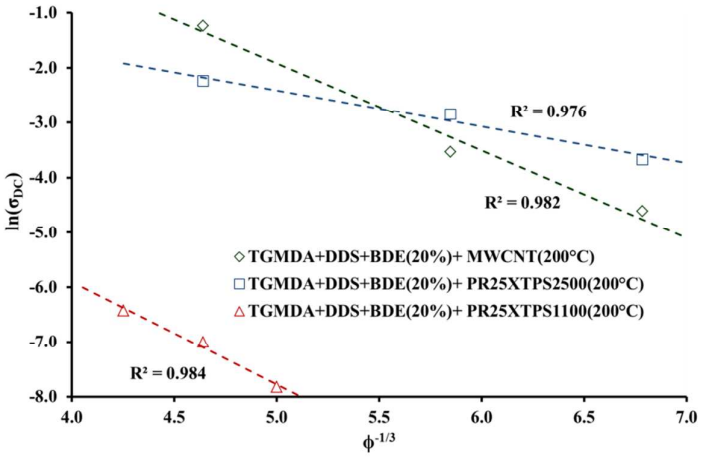

Fig. 14- Plot of the log of conductivity against □$^{-1/3}$.

The dashed line is a fit of the DC data to Eq. (4), the value of R^2 very close to 1 is indicative that the tunneling effect is the involved conduction mechanism. This supports the idea that the current is limited by potential barriers between nanotubes due to the resin coating, or conductivity above the percolation threshold depends largely on the interaction between the matrix and the filler and not on the conductivity of the filler.

Theoretical and experimental studies available in the literature [39,44-48] put in evidence the correlations between material characteristics (polymeric matrices, CNT type) and production process parameters, (synthesis method, treatment, etc.) with the electrical performances of the resulting composites. In particular, a previous work [49], concerning the influence of the cure temperature of the resin, has put in evidence that quite similar values of electrical conductivity can be obtained for the samples cured at 180 and 200°C. In fact, from the analysis of the Fig. 13 it is possible to note that the conductivities of the samples TBD-MWCNT(0.32%)(cured at 200°C) and TBD-MWCNT(0.32%)(cured at 180°C) are 0.029 S/m and 0.023 S/m respectively. The EPT for the composites filled by MWCNT and heat-treated CNFs (PX25XTP2500), falls in the range [0.1,0.32]%wt. Instead, for the composite filled by as-received CNFs (PR25XTP1100) the electrical percolation threshold is detected in the range [0.64, 0.80]%wt.

The remarkable difference in the EPT between the two type of nanofibers may be attributed to the different morphological feature and the high structural integrity of the heat-treated filler, as highlighted in the Section 3.1.

As it concerns the geometrical aspects, the theoretical prediction of the EPT for randomly-dispersed hard particles (of cylindrical shape) can be obtained with reference to the excluded volume theory associated to these objects [50]. According to this theory, the EPT of a composites filled with cylindrical conductive particles of diameter W and length L can be estimated as the inverse of the Aspect Ratio (AR=L/W).

For the as-received CNFs, having L=[20,200] μm and W=[125,150] nm, as reported in the manufacturer data-sheet, this theory indicates EPT less than 0.75% (i.e. the EPT obtained for L at minimum and W at maximum value respectively), a value which is very close to the experimentally detected (i.e. $EPT_{PR25XTPS1100} \in [0.64,0.8]\%$). Instead a lower electrical percolation threshold is observed for the heat-treated CNFs-based composite.

One plausible reason could be attributed to the thermal treatment that leads to the alignment of the fibers while the increased structural order induced by the graphitization of the fibers confers to them an higher rigidity, as conformed by the SEM images of Fig.10 and Fig.11.

This involves an increase of the "equivalent length" of the CNFs which determine a higher value of the AR and, as a consequence, a lower EPT.

The same mechanism may also justify the higher conductivity of heat-treated CNF for the same filler concentration. In fact, a larger number of electrical contacts can be produced by the longer, straight heat-treated fibers.

Therefore, the electrical experimental results confirm the strong influence of the different filler-resin interactions on the final electrical performance of the composites (i.e. electrical percolation threshold and conductivity at high filler loading).

The use of heat-treated CNFs rather than the more expensive and hard to disperse (especially for high concentrations) CNTs, could be an advantageous alternative for the production of conductive polymers satisfying also mechanical and thermal constraints required by the different applications.

3.5.2. Dielectric properties of the resin

The measurements of dielectric properties of the neat resins and of filled ones are required in order to achieve a compact and reliable design of electromagnetic shielding (EMI or RFI) and structural components for the automotive, aviation and aerospace applications.

The permittivity of the unfilled resins are measured in the range of [0.1-100] kHz. During the measurements, the temperature was kept constant at room temperature, therefore its possible influence can be considered negligible.

The real part (ε_r) of the complex effective permittivity of the samples based on TGMDA epoxy formulation with and without BDE diluent (labeled as TGMDA+DDS+BDE(20%)(200°C) and TGMDA+DDS(200°C), respectively), and of the sample based on DGEBA epoxy formulation (labeled as DGEBA+DDS) are shown in Fig.15. There is a slight decrease in the effective permittivity of the three different resins with increasing frequency in the entire measured frequency range.

Generally, in an epoxy resin system, the permittivity is characterized by the number of dipoles present in the structure and by their capability to orient under an applied electric field [51-52].

As in the epoxy chain, most of them can be oriented at low frequency. Thus, in the lower frequency range, the epoxy composites tend to show their highest value of permittivity due to the free dipolar functional groups and/or an interfacial polarization due to the presence of the conducting phase. When the frequency of the applied voltage increases, both mechanisms become negligible and the permittivity progressively decreases. The two TGMDA based systems are characterized by a relative permittivity (around 4) similar to what it has been found for another thermosetting resin (LY556) based on bisphenol-A cured with the hardener HY917 (anhydride type hardener) [53]. The DGEBA based system shows instead a higher value (>5). In the case of this last sample we performed the measurements to obtain a sample cured in the same condition of the TGMDA based systems (with a stoichiometric amount of DDS and using the same curing cycle).

The similar behavior of the two TGMDA systems is reasonably due to similar electrical polarization effects. A clear difference is evident for the DGEBA based system, which exhibit a higher electrical polarization. The dipole moments contribute to the polarization mechanisms in the epoxy resins which in turn influence their permittivity. The density of such dipolar groups in a cured epoxy system can be significantly different due to the nature of epoxy precursors and hardeners. Therefore, this occurrence could justify the discrepancy in the value of the permittivity of the two kinds of resin.

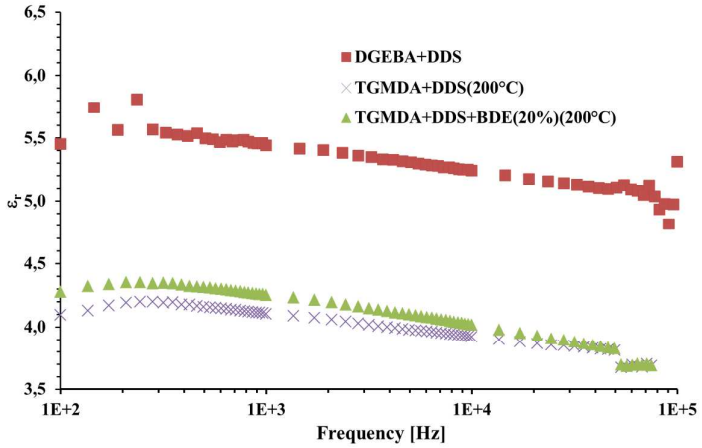

Fig. 15 - AC behavior of the relative electric permittivity for the TGMDA epoxy formulations (with and without diluent) compared with the formulation based on DGEBA at T=30°.

Moreover, the electrical conductivity is investigated as a function of the frequency in the range [1-100] kKHz. Regardless of the chemical formulation of the resin, the electrical conductivity (Fig.16) is typical of an insulator material.

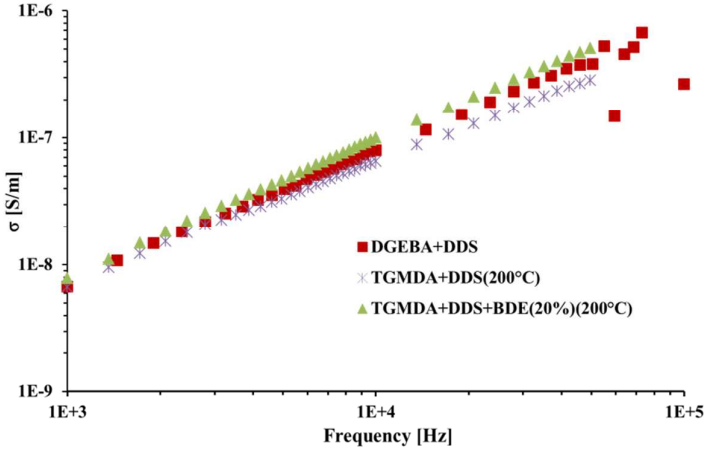

Fig. 16 - AC behavior of the electrical conductivity for the TGMDA epoxy formulations (with and without diluent) compared with the formulation based on DGEBA at T=30°.

The AC conductivity is generally dominated by the dielectric losses, rather than by the charge transport inside the material. The losses are associated to the part of the energy of the applied field which is dissipated as heat due to the "friction" between the molecules that are perturbed from their equilibrium condition by the applied electric field and forced to a continuous orientation. For this reason the ac conductivity increases as the frequency increases [54].

The values for the different systems are of the same order of magnitude and vary from about 10ns/m at 100Hz to about 1μS/m at 100kHz.

3.5.3. Impedance spectroscopy of nanocomposites

Detailed studies of *ac* electrical properties play an important role in the characterization of the nanocomposites for design and performance optimization purposes. The impedance spectroscopy (IS) is classically adopted tool for this aim. This technique is based on analyzing the ac response of the impedance parameters of a material to a sinusoidal stimulus as a function of the frequency. In this study the impedance ($\dot{Z}$) is represented by its magnitude ($|Z|$) and phase (φ).

This technique enables to detect the changing electrical response of the samples, and, for composites with conducting inclusions, the insulator to conductor transition. In particular, a critical frequency, *fc* [24] can be found where the frequency-independent behaviour changes to a frequency-dependent one.

The most commonly used model of a physical system involving these *ac* electrical parameters can be represented by a R_pC_p parallel electrical circuit. The relations between the impedance parameters and the electrical parameters of the equivalent circuit are:

$$|z| = \frac{R_p}{\sqrt{1+\omega^2 R_p^2 C_p^2}}, \qquad \varphi = atan(\omega R_p C_p) \tag{5}$$

where $\omega=2\pi f$ is the angular frequency and f is the frequency.

Therefore, the impedance spectroscopy of *ac* electrical behavior of neat resin and nanofilled resins is presented. The aim is to investigate how the addition, in different concentrations, of nanoparticles and their conducting behavior alters the electrical properties of the resulting materials. The results highlight a strong influence of the nanofiller nature on the electrical properties especially in terms of electrical percolation threshold (EPT) and electrical conductivity beyond the EPT. Among the analyzed nanofillers, the highest electrical conductivity is obtained by using multiwall carbon nanotubes (MWCNTs) and heat-treated carbon nanofibers (CNFs).

The frequency analysis of the composites is carried out by considering three filler concentrations [0.05, 0.32 and 1]% wt. These concentrations are chosen since 0.05 wt% is a value below the percolation threshold for all the three types of fillers, 0.32 wt% is a loading close to the

percolation threshold for the nanotubes (MWCNT) and the heat treated fibers (TPS2500) and finally 1% wt is a concentration fairly above the threshold for all composites regardless of the type of filler.

Fig.17 shows the plots of the magnitude of the normalized impedance *(*$|Z_{norm}|=|Z|*d/A$ in *Ω/m* where *d* is the thickness of the sample and *A* is the area of the electrode) and relative phase angle (degree) as function of the frequency.

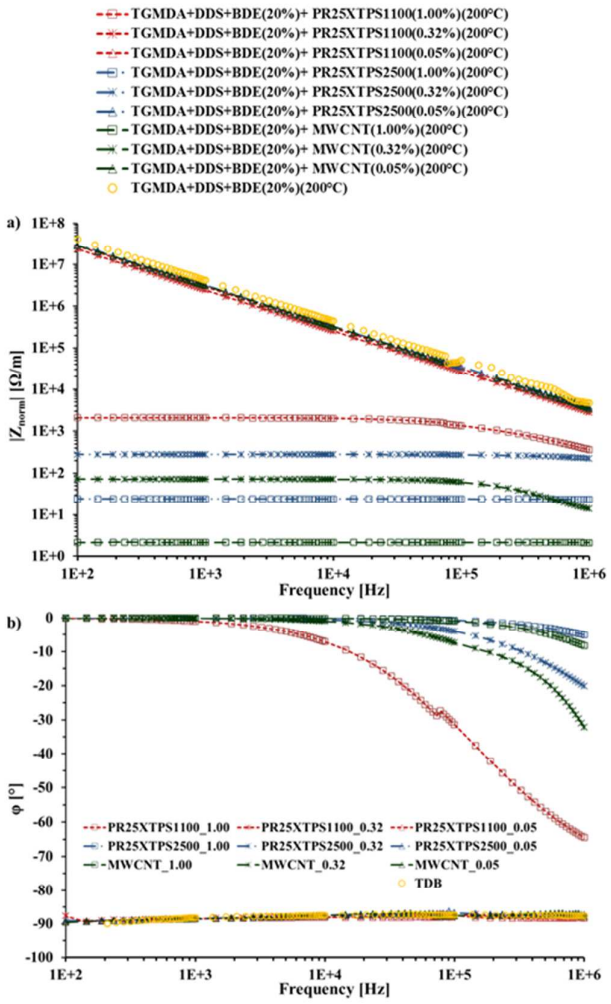

Fig. 17- Normalized impedance: a) and phase angle b) vs. frequency.

For the composites below the percolation threshold the $|Z_{norm}| \propto 1/f$ (in log-log scale is a straight line) and $\varphi \simeq -90°$, as for a typical insulating material, are strictly close to the behavior of the neat resin (yellow marker).

Instead, for the composite above the percolation threshold, it is interesting to note that both the modulus and phase exhibit a constant value until the frequency reaches a critical value f_c after which it decreases highlighting that at high frequency the electrical behavior of the composite is dominated by the capacitance of the system.

This aspect is most noticeable from the Fig.18 which shows the plots of $|Z_{norm}|$ and φ related to composites above the percolation threshold.

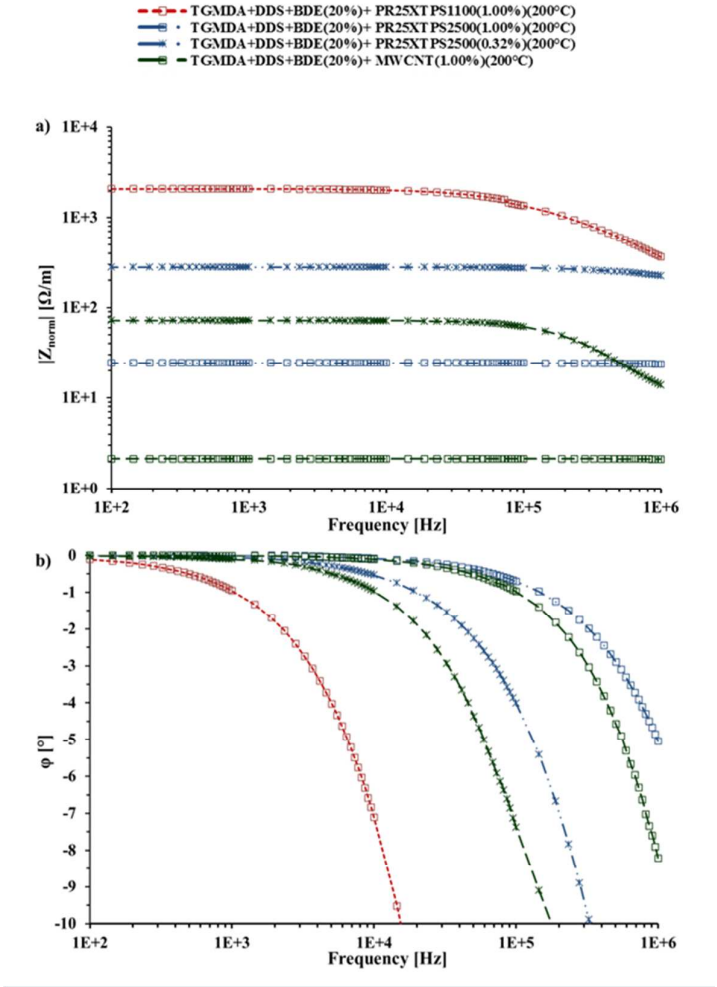

Fig. 18- a) $|Z_{norm}|$ and b) φ vs frequency for composites at filler loadings beyond percolation threshold.

At the same concentration, the composite made with MWCNT presents the lowest value of normalized impedance. In fact, the value of $|Z_{norm}|$ for the MWCNT is about one order of magnitude lower than that obtained with the heat-treated CNFs and 3 orders compared to as received CNFs, for the 1% concentration. Instead, the difference is about one order of magnitude for the concentration to 0.32% between MWCNTs and heat-treated CNFs.

As regards the frequency-dependent behavior it becomes less pronounced and the characteristic frequency f_c shift forward slightly with increasing filler loading indicating a transition of the material from a resistive-type to capacitive one according to the so called *universal dynamic response model* suitable to describe the electrical behavior in many disordered solids. [55-57]

This critical frequency is strictly correlated to the tunneling effect between carbon nanotubes in which both the (tunneling) distance and the height of energy barrier are somehow altered with respect to the stationary condition by the frequency of the applied electrical field. Synthetically, frequencies greater than this critical value (f_c) lead to a decrease of these parameters that in turn modulate the tunneling effect and consequently the electrical performance of the composites. [24]

However, the value of f_c is greater for the composites loaded with heat-treated CNFs compared to those with MWCNTs, as it is evident in Fig. a. This distinction is particularly evident in Fig. b, where it is possible to observe that, for a given frequency, the value of the filler loading for the composite PR25XTPS2500 is lower than that of the composite with MWCNT.

This suggests that the composites with heat-treated CNFs are characterized by a purely resistive behavior in a wider frequency range compared to that exhibited by other filled-composites. This interesting topic will be the object of a forthcoming paper where the behavior of the composites will be investigated in a wider frequency range.

4. Concluding remarks

We have formulated, prepared and characterized an epoxy resin mixture based on a tetrafunctional epoxy precursors, the TetraGlycidyl-MethyleneDiAniline (TGMDA). The presence of reactive diluent 1,4-Butandioldiglycidylether in the epoxy mixture reduces the sorption at equilibrium of liquid water (C_{eq}) of about 35%. This percentage is very relevant for epoxy mixtures to apply in the aeronautics because absorbed moisture reduces the matrix-dominated mechanical properties. Absorbed moisture also causes the matrix to swell. This

swelling relieves locked-in thermal strains from elevated temperature curing. These strains can be large and large panels, fixed at their edges, can buckle due to the swelling strains. In addition, during freeze-thaw cycles, the absorbed moisture expands during freezing and can crack the matrix. In addition, during thermal spikes, absorbed moisture can turn to steam. When the internal steam pressure exceeds the flatwise tensile strength of the composite, the laminate will delaminate. The reduction in the water absorption was also found for nanofilled epoxy mixtures formulated to increase the electrical conductivity. The presence of the reactive diluent allows to reach higher curing degree compared to the epoxy precursor alone providing an efficient strategy for energy-saving.

The morphological feature of the nanofillers has proven to play a relevant role in determining the electrical properties of the analyzed nanofilled resins. The composites obtained with heat treated CNF are characterized by the lowest value, among all considered systems, of the percolation threshold and by a dc conductivity of the same order of the more expensive and hard to disperse (especially for high concentrations) CNTs. Also the frequency behavior of the composites put in evidence that CNF composites could be advantageously employed for the production of materials for aeronautic components since they are also suitable for managing mechanical and thermal constraints required by such applications.

ACKNOWLEDGEMENTS

The research leading to these results has received funding from the European Union Seventh Framework Programme FP7/2007-2013 under grant agreement n° 313978.

References

[1] Lopes J.C.O. Materials selection for aeronautical structural application. Ciência Tecnologia dos Materiais 2008;20(3/4):78–82.
[2] Z. Huda, P. Edi. Materials selection in design of structures and engines of supersonic aircrafts: A review. Materials and Design 2013;46:552–560.
[3] James C. Williams, Edgar A. Starke, Jr. Progress in structural materials for aerospace systems. Acta Materialia 2003;51:5775–5799.
[4] Bellucci S., Balasubramanian C, Micciulla F., Rinaldi G. CNT composites for aerospace applications. Journal of Experimental Nanoscience 2007; 2:193-206.
[5] Mangalgiri P. D. Composite materials for aerospace applications. Bulletin of Materials Science 1999; 22(3):657-664.

[6] Wang X., Yong Z. Z., Li Q. W., Bradford P. D., Liu W., Tucker D. S., Cai W., Wang H., Yuan F. G., Zhu Y. T. Ultrastrong, Stiff and Multifunctional Carbon Nanotube Composites. Materials Research Letters 2012; 1:1–7.
[7] Song K., Zhang Y., Meng J., Green E.C., Tajaddod N., Li H., Minus M. L..Structural Polymer-Based Carbon Nanotube Composite Fibers: Understanding the Processing–Structure–Performance Relationship. Materials 2013; 6:2543-2577
[8] Taczak M.D. A Brief Review of Nanomaterials for Aerospace Applications: Carbon Nanotube-Reinforced Polymer Composites- The MITRE Corporation, MCLean Virginia, May 2006.
[9] Rea S., Linton D., Orr E., McConnell J. Electromagnetic Shielding Properties of Carbon Fibre Composites in Avionic Systems. Microwave Review 2005; 11(1):29-32.
[10] De Rosa I.M., Sarasini F., Sarto M.S., Tamburrano A. EMC Impact of Advanced Carbon Fiber/Carbon Nanotube Reinforced Composites for Next-Generation Aerospace Applications IEEE Transaction on Electromagnetic Compatibility 2008; 50 (3):556-563.
[11] Iijima S. Helical microtubules of graphitic carbon. Nature 1991;354(6348):56-8.
[12] Andrews R, Weisenberger MC. Carbon nanotubes polymer composites. Current Opinion in Solid State and Materials Science 2004;8(1):31-7.
[13] Coleman JN, Khan U, Gun'ko YK. Mechanical reinforcement of polymers using carbon nanotubes. Adv Mater 2006;18(6):689–706.
[14] Moniruzzaman M, Winey KI. Polymer nanocomposites containing carbon nanotubes. Macromolecules 2006;39(16):5194–205.
[15] Coleman JN, Khan U, Blau WJ, Gun'ko YK. Small but strong: a review of the mechanical properties of carbon nanotube-polymer composites. Carbon 2006;44(9):1624–52.
[16] Xie XL, Mai YW, Zhou XP. Dispersion and alignment of carbon nanotubes in polymer matrix: a review. Mater Sci Eng R 2005;49(4): 89–112.
[17] Guadagno L, Vertuccio L, Sorrentino A, Raimondo M, Naddeo C et al. Mechanical and barrier properties of epoxy resin filled with multi-walled carbon nanotubes. Carbon 2009;47(10):2419-30.
[18] Guadagno L, De Vivo B, Di Bartolomeo A, Lamberti P, Sorrentino A et al. Effect of functionalization on the thermo-mechanical and electrical behavior of multi-wall carbon nanotube/epoxy composites. Carbon 2011;49:1919-30.
[19] Sandler JKW, Kirk JE, Kinloch IA, Shaffer MSP, Windle AH. Ultra-low electrical percolation threshold in carbon-nanotube-epoxy composites**.** Polymer 2003;44(19):5893-99.
[20] Khare R, Bose S. Carbon nanotube based composites-a review. Journal of Minerals & Materials Characterization & Engineering 2005;4(1):31-46.
[21] De Vivo B, Guadagno L, Lamberti P, Raimo R, Sarto MS et al. Electromagnetic properties of Carbon NanoTube/epoxy nanocomposites. Extended abstracts, IEEE Conference Proceeding, International Symposium on Electromagnetic Compatibility - EMC Europe 2009, Athens (Greece), 11-12 June 2009; p.1-4, DOI 10.1109/EMCEUROPE.2009.5189674.
[22] Guadagno L, Naddeo C, Vittoria V, Sorrentino A, Vertuccio L et al. Cure Behavior and Physical Properties of Epoxy Resin Filled with Multiwalled Carbon Nanotubes. Journal of Nanoscience and Nanotechnology 2010;10(4):2686-93.
[23] Iannuzzo G, Calvi E, Russo S, Guadagno L, Naddeo C et al. Smart Carbon Nanotubes/Epoxy Composite Materials for Advanced Aerospace Applications. Extended abstracts, SAMPE Europe 29th Int. Conf. and Forum 2008, Paris (France) , 31 March-2 April 2008:246-51.
[24] Connor T, Roy S, Ezquerra TA, Balta-Calleja FJ. Broadband AC conductivity of conductor-polymer composites. Phys Rev B 1998; 57(4):2286-94.
[25] Mdarhri A, Carmona F, Brosseau C, Delhaes P. Direct current electrical and microwave properties of polymer-multiwalled carbon nanotubes composites. J Appl Phys 2008; 103: 054303(1)-054303(9).
[26] Maas TA. Optimalization of processing conditions for thermosetting polymers by determination of the degree of curing with a differential scanning calorimeter. Polym Eng Sci 1978;18:29–32.
[27] Pappalardo L T. DSC Evaluation of B- Stage Epoxy-Glass Prepregs for Multilayer Boards. Soc Plast Eng 1974; 20:13–16.
[28] Sanjana, Z. N.; Sampson, R. N. Measuring the degree of cure of multilayer circuit boards. Insul Circuits 1981; 27:87–92.
[29] Horie K, Hiura H, Sawada M, Mita I, Kambe H. Calorimetric investigation of polymerization reactions. III. Curing reaction of epoxides with amines. J Polym Sci Part A-1: Polym Chem 1970; 8:1357–72.

[30] Edwards, G, Ng QY. Elution behavior of model compounds in gel permeation chromatography. J Polym Sci [C] 1968; 21:105–117.
[31] Maxwell I, Pethrich RA. Dielectric studies of water in epoxy resins. J Appl Polym Sci 1983;28:2363-79.
[32] Liu W, Hoa SV, Pugh M. Fracture toughness and water uptake of high-performance epoxy /nanoclay nanocomposites – Composites Sci and Techn 2005; 65:2364 - 73.
[33] Li L, Yu Y, Wu Q, Zhan G, Li S. Effect of chemical structure on the water sorption of amine-cured epoxy resins. Corrosion Science 2009;51:3000-3006.
[34] Sarti GC. Solvent Osmptic Stresses and the prediction of case II transport kinetics, Polymer 1979, 20:827.
[35] Sarti GC, Apicella A. Non-equilibrium glassy properties and their relevance in case II transport kinetics, Polymer 1980; 21:1031.
[36] Thomas NL, Windle AH. A deformation Model for case II Diffusion, Polymer 1980;21:613.
[37] Endo M, Kim YA[a], Hayashi T, Yanagisawa T, Muramatsu H et al. Microstructural changes induced in "stacked cup" carbon nanofibers by heat treatment. Carbon 2003; 41:1941- 47.
[38] Guadagno L, Raimondo M, Vittoria V, Lafdi K, De Vivo B et al. Role of the carbon nanofiber defects on the electrical properties of CNF-Based resins. Nanotechnology 2013; 24: 305704 (10pp).
[39] Bauhofer W, Kovacs JZ. A review and analysis of electrical percolation in carbon nanotubes polymer composites. Composite Science and Technology 2009;69:1486–98.
[40] De Vivo B, Guadagno L, Lamberti P, Sorrentino A, Tucci V et al. Comparison of the Physical Properties of Epoxy-Based Composites Filled with Different Types of Carbon Nanotubes for Aeronautic Applications. Adv Polym Tech 2012;31:205–218.
[41] Mclachlan DS, Chiteme C, Cheol P, Wise KE, Lowther SE et al. AC and DC Percolative Conductivity of Single Wall Carbon Nanotube Polymer Composites. J Polym Sci Part B: Polym Phys 2005; 43:3273–3287.
[42] Sandler JKW, Kirk JE, Kinloch IA, Shaffer MSP, Windle AH.Ultra-low electrical percolation threshold in carbon-nanotube–epoxy composites. Polymer 2003;44(19):5893–9.
[43] Kilbride BE, Coleman JN. Experimental observation of scaling laws for alternating current and direct current conductivity in polymer-carbon nanotube composite thin films. J Appl Phys 2002; 92(7):4024-30
[44] Spinelli G, Giustiniani A, Lamberti P, Tucci V, Zamboni W. Numerical Study of Electrical Behaviour in Carbon Nanotube Composites. Int J Appl Electrom 2012; 39: 21-27.
[45] Hu N, Masuda Z, Yan C, Yamamoto G, Fukunaga H, et al. The electrical properties of polymer nanocomposites with carbon nanotube fillers. Nanotechnology 2008;19: 21571-80.
[46] Eken E, Tozzi EJ, Klingenberg DJ, Bauhofer WJ. A simulation study on the combined effects of nanotube shape and shear flow on the electrical percolation thresholds of carbon nanotube/polymer composites. Appl Phys 2011; 109:084342-9.
[47] Li C, Chou TW. Dominant role of tunneling resistance in the electrical conductivity of carbon nanotube–based composites. Appl Phys Lett 2007; 90(22): 223114-3.
[48] Guadagno L, Raimondo M, Vittoria V, Lafdi K, De Vivo B et al. Role of The Carbon Nanofiber Defects On The Electrical Properties of CNF-Based Composites. International Symposium on Aircraft Materials (Fez, Morocco) 2012:1-8
[49] Guadagno L, Vertuccio L, Naddeo C, De Vivo B, Spinelli G et al. Electrical and dynamic mechanical properties of MWCNTs/Epoxy composite for high performance aerospace applications 15TH European Conference On Composite Materials (Venice, Italy) 2012; 24-28.
[50] Balberg I, Anderson CH, Alexander S, Wagner N. Excluded volume and its relation to the onset of percolation. Phys. Rev. B 1984;30:3933.
[51] Sheppard Jr. NF, Senturia SD. Chemical interpretation of the relaxed permittivity during epoxy resin cure. Polym Eng Sci 1986;26:354–57.
[52] Eloundou J P. Dipolar relaxations in an epoxy–amine system. European Polymer Journal 2002;38:431–438.
[53] Wang Q, Chen G. Effect of nanofillers on the dielectric properties of epoxy nanocomposites. Adv Mater Res 2012;1(1): 93-107
[54] Murphy EJ, Morgan SO. The Dielectric Properties of Insulating Materials, III Alternating and Direct Current Conductivity. Bell System Technical Journal 1939;18:502-537.
[55] Dyre JC. The random free-energy barrier model for ac conduction in disordered solids. J Appl Phys 1988; 64:2456-68.
[56] Dyre JC, Schrøder TB. Universality of ac conduction in disordered solids. Rev Mod Phys 2000;72: 873-92.
[57] Jonscher AK. The universal dielectric response: Part I. IEEE Electr Insul M 1990; 6: 16 - 22.

FIGURE CAPTIONS

Fig. 4 - DSC curves of: a) the uncured and cured epoxy resin TGMDA+DDS (without reactive diluent) on the left side, and b) the uncured and cured epoxy mixture TGMDA+DDS+BDE(20%)(TGMDA with reactive diluent/DDS) on the right side.

Fig. 5 - DSC curves of: the uncured epoxy mixture TGMDA+DDS+BDE(20%), and the same epoxy mixture cured by two different curing cycles.

Fig. 6 - Storage modulus (MPa) (at the top), and Loss factor (tanδ) (at the bottom) of the pure epoxy and the composites 0.32 wt% MWCNTs solidified up to 180 and 200°C respectively.

Fig. 4 - The concentration at time (C_t) as a function of the time (hours) of the epoxy resin (without BDE), and the epoxy mixture containing the diluent.

Fig. 5 - C_t/C_{eq} against the square root of time normalized for the thickness d of unfilled and nanofilled mixtures.

Fig. 6 - Thermogravimetric curves in air of: a) the uncured and cured unfilled epoxy resin TGMDA/DDS (without reactive diluent) on the left side, and b) the reactive diluent BDE on the right side.

Fig. 7 - Thermogravimetric curves in air of : a) the uncured and cured unfilled epoxy mixture TGMDA+DDS+BDE(20%) (TGMDA with reactive diluent/DDS) on the left side, and b) the same epoxy formulation nanofilled with a percentage of 0.32% of MWCNTs on the right.

Fig. 8- Fracture surface SEM images of the nanofilled epoxy composites at loading rate of Sample A) 0.64, Sample B) 0.32 and Sample C) 0.05 per cent by weight of CNTs.

Fig. 9 - TEM image of Sample B (epoxy resin at loading rate of 0.32 per cent by weight of CNTs).

Fig. 10- Fracture surface SEM images of the nanofilled epoxy composites at loading rate of 0.64 per cent by weight: as received CNFs filled resin is on the top, heat-treated CNFs filled resin is on the bottom.

Fig. 11- Fracture surface SEM images of the nanofilled epoxy resins at loading rate of 1% by weight: as received CNFs filled resin is on the top, heat-treated CNFs filled resin is on the bottom.

Fig. 12 - Fracture surface SEM images (enlargement) of the nanofilled epoxy resins at loading rate of 1% by weight: as received CNFs filled resin is on the top, heat-treated CNFs filled resin is on the bottom.

Fig. 13 - DC volume conductivity of the nanofilled composites as a function of the nanofiller concentration.

Fig. 14- Plot of the log of conductivity against $\square^{-1/3}$.

Fig. 15 - AC behavior of the relative electric permittivity for the TGMDA epoxy formulations (with and without diluent) compared with the formulation based on DGEBA at T=30°.

Fig. 16 - AC behavior of the electrical conductivity for the TGMDA epoxy formulations (with and without diluent) compared with the formulation based on DGEBA at T=30°.

Fig. 17- Normalized impedance: a) and phase angle b) vs. frequency.

Fig. 18- a) $|Z_{norm}|$ and b) φ vs frequency for composites at filler loadings beyond percolation threshold.